High Energy Physics and Nuclear Physics
Volume 12, No. 4

The Study of the Dissipation Process and the Nucleon Transfer Produced by the 80.9 MeV ^{16}O on ^{27}Al

Yin Xu, Shen Wenqing, Zhu Yongtai, Feng Enpu, Wang Qi, Xie Yuanxiang, Zhan Wenlong and Li Songlin

(Institute of Modern Physics, Chinese Academy of Sciences, Lanzhou)

The three-fold differential cross sections $d^3\sigma/dAdZdE$ of the projectile-like fragment produced by the 80.9 MeV ^{16}O on ^{27}Al have been measured, using a time of flight system with ΔE-E telescope. The relation between the dissipation process and the nucleon exchange that appears in the reaction has been discussed.

1. INTRODUCTION

In heavy ion reaction, with the lengthening of interaction time and the increase of overlapping between the projectile and the target, various degrees of freedom in the entrance channel will relax in order. The composite system either decays into ground state by emitting light particles or exchanges a few nucleons, dissipating most or all the kinetic energy, breaking up into two asymmetric fragments and maintaining part of the "memory" of the entrance channel. The former type of interaction is called complete fusion, the latter is called deep inelastic collision (DIC).

In the light system, the research on the reactions of ^{16}O bombarding ^{27}Al at some energies, for example, with the incident energies at 90 MeV, 100 MeV [1], 88 MeV [2], 70 MeV, 60 MeV [3], has indicated that the deep inelastic process appears above 70 MeV. Its cross sections increase with the rise of the incident energy. A study of the reaction ^{16}O + ^{27}Al at 80.6 MeV by Shen Wenqing et al. of IMP was reported, in which the charge numbers of products were identified, and the potential energy surface effect and the relaxation

Received on January 26, 1987.

process were analyzed. However, the mass and charge numbers of the products could not be identified simultaneously [4,5].

We have designed and tested a heavy ion time of flight device with a ΔE-E telescope-TOF system which has been used to identify the mass and charge numbers of the products simultaneously for the above-mentioned reaction. The triple differential cross sections $d^3\sigma/dAdZdE$ as a function of energy, mass and charge numbers of the reaction products have been measured. Therefore, the relation between the dissipative process and the exchanging nucleons, the correlation between neutron and proton exchange, the exchange dominance between them in different region of excitation energy and the effect which the potential energy surface acts on nucleons exchange have been investigated.

2. EXPERIMENTAL SET-UP AND METHOD

The beam energy of the ^{16}O projectiles was 87.5 MeV. A self-supporting Al target was used with a thickness of 0.76 mg/cm^2. In order to lessen the contamination of the light elements, a scattering chamber in which the oil contamination could be reduced with a special measure at IMP was used [6] and the target surface was cleaned with the electron sputtering method. The beam passed through a 1.94 mg/cm^2 Ni foil, which separated the scattering chamber from the system of cyclotron, and finally its energy at half of the target thickness reached 80.9 MeV. The ratio of the energy in C.M. system to the coulomb barrier (E_{cm}/B) is about 3.1. The distribution of the reaction products in (ΔE, E, T) three-dimensional space was measured by means of the TOF system with ΔE-E telescope. Z numbers of reaction products were determined by ΔE, E and the numbers of M (or A) by E, T. The Z, $M(A)$, energy E of the products at a certain angle were obtained simultaneously.

A mixture of gases Ar(90%) + CH (10%) was filled into the ΔE-detector. Its pressure was 37 Torr and corresponded to a thickness of 0.795 mg/cm^2. The E-detector was a Si(Li) detector. The distance of the flight path of the TOF system was 127.9 cm. The start time signal t_0 was provided by a "zero-time" device that consisted of a scintillation film and a photo-multiplier. The stop time signal t was given by the E-detector. The time resolution of the TOF system was about 500 ps. Then the mass resolution $\Delta M/M$ was 1%, and the charge resolution $\Delta Z/Z$ 3.5%. The solid angle subtended by the detector system was 5×10^{-5} sr. The beam current was measured by a calibrated current integrator. Data were acquired in a plurimat-N multi-parameter data acquisition system. Data were recorded event by event on tapes. The off-line data analysis was done on a Wang-220VS computer and an IBM-PC/AT computer, separately.

A and E of the products were measured at $\theta_L = 10°$–$60°$. In fact, simultaneous identifications of Z and A as well as E measurement were done at 14.5° only.

3. EXPERIMENTAL RESULTS AND ANALYSIS

M distributions of the products at three angles 16°, 25°, 40° are shown in Fig. 1. There are two kinds of products, projectile-like fragments and target-like fragments in Fig. 1. They originate from the products with the masses near projectile and target respectively and maintain individual properties. Kinetic energies of heavy fragments at large angle are

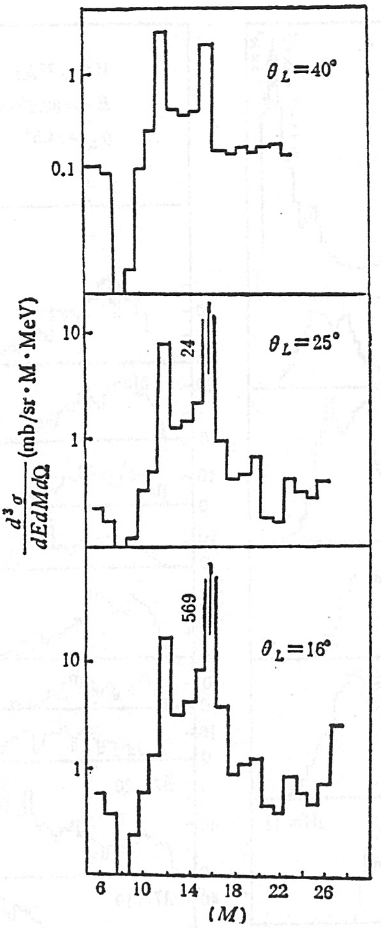

FIG. 1 M distributions at θ_L = 16°–40°. Coordinate is logarithm scale; digits at arrow are elastic scattering cross sections.

almost dissipated, therefore the flight time is so long that this part of events cannot be recorded in the data acquisition system.

In deep inelastic scattering reaction, the mass distribution, the charge distribution and the neutron distribution are of Gaussian form. In Fig. 1 only the target-like fragments whose masses are less than that of the target were measured because of the detector threshold. From the measurement the data for $M \leq 27$ were extracted. The distributions of the projectile-like fragments deviate slightly from the Gaussian one. A deep valley of $M = 8$ corresponds to ^8Be, which is unstable and decays into two α-particles very fast. The peak of $M = 12$ comes from the exchanging nucleons and also possibly from the quasi-elastic break-up. In the interaction with the target the recoiling nucleus with high energy will break up as $^{16}O \rightarrow \alpha + {}^{12}C$. Looking at the M-E energy spectra at θ_L = 14.5° (Fig. 2), the maximum energy and the cross section of $M = 12$ are larger than that of the products in the vicinity. The angular distributions integrated over the energy spectra of products at different angles show that their slopes are very steep and they are peaked at forward angle

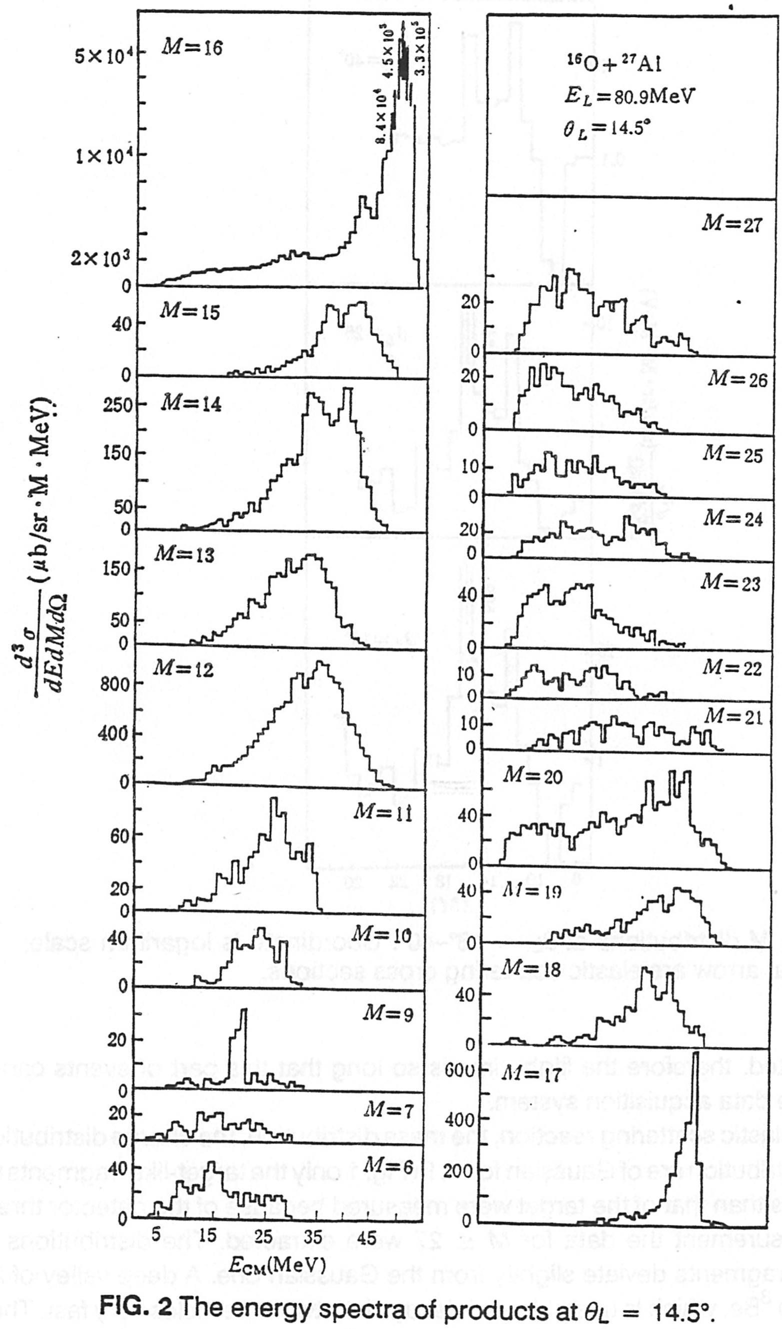

FIG. 2 The energy spectra of products at $\theta_L = 14.5°$.

for the projectile-like nuclei. The angular distributions of the products far from the projectiles consist of two components which have different slopes: forward peaked in small angles to more flat in backward angles.

Both the mass distributions which get broader and broader with increasing angle and the characteristics in angular distributions mentioned above indicate that with interaction time becoming longer and nucleon exchange increasing gradually, the kinetic energy dissipation becomes larger, the cross sections of the quasi-elastic component decrease and then the reaction develops towards deep inelastic scattering process.

Various average values and the corresponding variances and correlated coefficient ρ as a function of the total kinetic energy loss are shown in Fig. 3. They have been defined as

$$\bar{A} = \frac{\sum_i A_i\sigma_{Ai}}{\sum_i \sigma_{Ai}}; \quad \sigma_A^2 = \frac{\sum_i (A_i - \bar{A})^2\sigma_{Ai}}{\sum_i \sigma_{Ai}}$$

$$\bar{Z} = \frac{\sum_i Z_i\sigma_{zi}}{\sum_i \sigma_{zi}}; \quad \sigma_z^2 = \frac{\sum_i (Z_i - \bar{Z})^2\sigma_{zi}}{\sum_i \sigma_{zi}}$$

$$\bar{N} = \frac{\sum_i N_i\sigma_{Ni}}{\sum_i \sigma_{Ni}}; \quad \sigma_N^2 = \frac{\sum_i (N_i - \bar{N})^2\sigma_{Ni}}{\sum_i \sigma_{Ni}}; \quad \rho = \frac{\sigma_A^2 - (\sigma_Z^2 + \sigma_N^2)}{2\sigma_Z\sigma_N}$$

here $N_i = A_i - Z_i$, which can be calculated from the measured mass number and the charge number.

Since Huizenga found the general relation between the total kinetic energy loss TKEL and the variance of the charge distribution, it has been adopted as a usual method to connect the energy dissipation between two nuclei and the exchanging nucleons. Therefore, σ_Z^2 (or σ_A^2, σ_N^2), as a function of TKEL, is obtained. It is very important for the study of the reaction mechanism. Various distributions obtained from the experiment all deviate from the Gaussian one. The method mentioned above reasonably reflects the average characteristics of the average value and the width which measure the drift and the diffusion property of the system.

Using data obtained from the experiment and the average value formula, the calculated mass average values $\bar{A}$, the charge average values $\bar{Z}$ and the neutron average values $\bar{N}$ all have the same trend of variation, that is, with TKEL or interaction time increasing, all these average values drift about 1 unit first downwards, then upwards.

Relations between the different variance of σ_A^2, σ_Z^2, σ_N^2 and TKEL are shown in Fig. 3. On the average, the second moments increase as TKEL increases. For small TKEL, various variances increase slowly with increasing TKEL. However, for large TKEL, variances change very fast with increasing TKEL.

The variance increasing first slowly and then fast with the increasing total kinetic energy loss is similar to the behaviour of the deep inelastic scattering in heavy system. For lighter system at low bombarding energy, except the effect of light particle emitted from the fragments, the nuclear structure and the odd-even effect, the diffusion process of nucleon plays an important role.

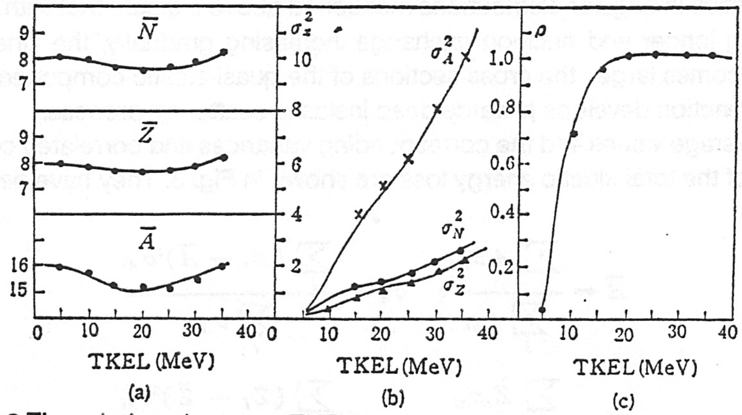

FIG. 3 The relations between TKEL and (a) average values (b) Variances (c) ρ.

The quantity σ_A^2/σ_Z^2 was used to describe the relation between neutron and proton exchange earlier on. Recently, a better quantity ρ is used instead. These two quantities are related by the following conditions:

$$\text{When } \rho = 0, \quad \sigma_A^2/\sigma_Z^2 \longrightarrow A_C/Z_C$$

$$\text{When } \rho = 1, \quad \sigma_A^2/\sigma_Z^2 \longrightarrow (A_C/Z_C)^2$$

$\rho = 0$ means the uncorrelated neutron and proton exchange, which corresponds to single nucleon transfer reaction or unexcited state mechanism. $\rho = 1$ means the completely correlation or maximum correlation of neutron and proton exchange. A_C and Z_C are mass and charge number of the composite system, respectively. The quantity ρ increases from 0 to 1 and σ_A^2/σ_Z^2 changes from a value more than $A_C/Z_C = 2.1$ to approximately $(A_C/Z_C)^2$ as dissipated energy increases from zero to maximum. The change of σ_A^2/σ_Z^2 and ρ deviates in small TKEL region. This is similar to the change in the reaction of some heavy systems. As some researchers have pointed out recently that it seems that the quantity σ_A^2/σ_Z^2 cannot describe the degree of correlation of the nucleon transfer completely, but expresses the degree of the neutron transfer being easier than the proton transfer. In some papers it was even considered as a scale of the shell structure effect at the injection point [7]. The process that the correlation coefficient changes from 0 to 1 with increasing dissipated kinetic energy indicates that the reaction evolves from quasi-elastic to deep inelastic process, then neutron and proton exchanging develops from uncorrelated mode at the early stage to completely correlated mode at the final stage.

Another physical quantity R is defined as

$$R = (\sigma_A^2/\sigma_Z^2)/(A_C/Z_C).$$

which is considered as the dominant degree of neutron exchange rather than proton exchange in the small excitation energy region. $R = 1$ means that the probabilities of neutron and proton exchange are the same. $R > 1$ and $R < 1$ correspond to the large probability of neutron exchange and that of proton exchange respectively.

The calculation indicates that as TKEL increases from 0 to 15 MeV, R is between 1.5-1.8 approximately. It means that in the small excitation energy region, neutron exchange is easier than proton exchange. In the large excitation energy region, since the changes of A_C/Z_C are connected with the change of the excitation energy, $R' = \sigma_A^2/\sigma_Z^2/(A_C/Z_C)^2$ can be used to describe the process. At large TKEL, for example, 25–40 MeV, $R' \approx 1.1$. This indicates that the probabilities of the neutron and proton exchange are almost the same in this region. This is consistent with the behaviour of the correlation coefficient ρ that when ρ changes from 0 to 1, the neutron proton exchange becomes from uncorrelated to completely correlated. At large TKEL, neutron proton exchange is completely correlated, the exchanging probabilities should be the same.

Various average values drift toward small values in the experiment. One main reason causing this kind of drift is that the system is acted on by the driving potential which goes to small gradient of the potential energy surface. Two dimensional and one dimensional graphs of the potential energy surface for $^{16}O + {}^{27}Al$ are given in Fig. 4. In the two dimensional potential energy surface (the average angular momentum in the region in which DIC takes place is equal to 32), the injection point is at $N = 8$, $Z = 8$. The lowest valley of the potential is at $N = 6$, $Z = 6$ from where the values of the contour gradually increase. In order to show the fine structure of the potential energy surface clearly, the driving potential including the shell effect is also given. In Fig. 4, the line LD is the LDM potential calculated by means of the liquid drop model without the shell effect. The dash line EM is the driving potential calculated by using the experimental mass table. PA is the EM's parabolic approximation which is obtained by least square fitting EM in $6 \le Z \le 9$ region.

If the structure effects is negligible, the composite system is forced by the LD potential to drift towards the minimum or the symmetric point of the potential energy surface, the average $\bar{Z}$ value increases from 8 to 10. The experimental observation shows that the first moment drifts toward small value by 1 unit. Considering the structure effect on potential, the minimum of the driving potential is no longer at the symmetric point of the LD potential

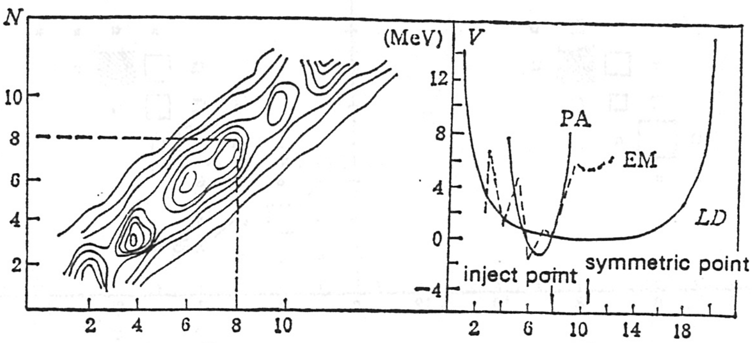

FIG. 4 One and two dimensional potential energy surface of $^{16}O + {}^{27}Al$ system.

and the LD potential should be replaced by the EM potential, which makes the first moment decrease by two units and arrive at the $^{12}_{6}C$ position and stabilize there finally. As a matter of fact, the experimental value is rather close to the valley of the PA potential.

With or without considering the structure effect, the experimental results about the first moment drift could not be fully understood. Actually, at small TKEL, the potential with the structure effect plays a role. Then, the temperature and the deformation of the dinuclear system increase with increasing TKEL. The shell effect is smeared out gradually in the large TKEL region, the LD potential plays an important role again. Probably this is the reason why various average values $\bar{A}, \bar{Z}, \bar{N}$ drift downwards first with increasing TKEL, then drift upwards at large TKEL.

Both (a) the yields of isotope products in *N-Z* plane, obtained from the TOF and the ΔE-E detector system, and (b) the yields of the corresponding isotope products calculated from the potential energy surface, are shown in Fig. 5 which illustrates the effect of the potential energy surface on nucleon transfer. In terms of the partial statistic equilibrium principle, the values of the potential energy surface for the different exit channel are used to calculate the corresponding yields $d(N,Z)$:

$$d(N, Z) \propto \exp(-V_{PES}(N, Z)/T)$$

here, T is a constant parameter related to the nuclear temperature. The potential energy surface can be calculated by

$$V_{PES}(N, Z) = V_{out} - V_{in}$$
$$= -Q_{gg} + V_{coul} + V_{rot}$$

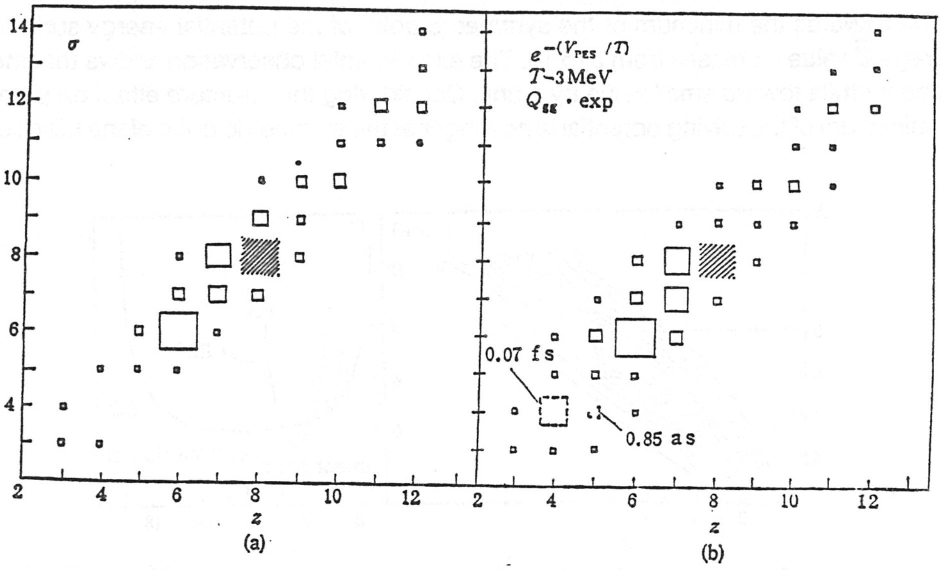

FIG. 5 (a) The measured yields of isotopes. (b) Yields of isotopes calculated from potential energy surface.

here V_{coul}-coulomb energy of the exit channel, V_{rot}-the rotating energy, $Q_{g\,g}$ is the Q-value of the ground state calculated with the nuclei mass table.

The area of each square represents the isotope yield normalized by the yield of ^{12}C. The selected nuclear temperature is 3 MeV. The shadow area corresponds to the elastic scattering process. The experimental results for most products are consistent with those calculated by the above-mentioned method, except for the products which have too short life-times to be measured in the experiment.

4. CONCLUSION

At the incident energy of 80.9 MeV, DIC component has been observed. With the interaction time evolving, the energy dissipation increasing gradually, and the nucleon exchange increasing, the system develops towards fully damping. At small TKEL, $\rho = 0$ the proton and neutron exchanges are uncorrelated, the quantity R shows $\sigma_A^2/\sigma_Z^2/(A_C/Z_C) > 1$, which indicates that the neutron exchange is easier than the proton exchange in the small excitation energy region. In strong damping, $\rho=1$, $\sigma_A^2/\sigma_Z^2 \longrightarrow (A_C/Z_C)^2 \doteq 4$, which means that the proton and neutron exchanges are completely correlated. Quantity $R' \to 1$, which indicates that the exchanging nucleons are correlated and the exchange probabilities are the same. Various average values drift towards small values, then towards large values with the interaction time increasing. This is because of the results of the potential energy surface with the shell effect strongly acting on, then, as TKEL continues to increase, the shell effect is smeared out gradually, at the same time the system is acted on by the potential energy surface without the shell effect. The observed yields of isotope products in the experiment are basically consistent with those calculated using the potential energy surface.

ACKNOWLEDGEMENTS

The authors would like to thank Volkswagen Seiftiung and Prof. R. Bock for their support and concern over our work.

REFERENCES

[1] T. M. Cormier et al., *Phys. Rev.* C13(1976), 682.
[2] T. Mikvmo et al., *Phys. Rev.* C21(1980), 620.
[3] M. Sato et al., *Phys. Rev.* C27(1983), 500.
[4] Shen Wenqing et al., *Physica Energiae Fortis Et Physica Nuclearis*, 3(1985), 332.
[5] Shen Wenqing et al., *Physica Energiae Fortis Et Physica Nuclearis*, 5(1985), 611.
[6] Zhu Yongtai et al., Annual Report of IMP (1981), 114.
[7] Wu Enjiu et al., Annual Report of IMP (1980), 44.